Spatially Correlated Rician-Faded Multi-Relay Massive MIMO NOMA Systems

Bibhor Kumar, Dheeraj Naidu Amudala, Rohit Budhiraja
Department of Electrical Engineering, IIT Kanpur India
{bibhork, dheeraja, rohitbr}@iitk.ac.in

ICC 2022 - IEEE International Conference on Communications | 978-1-5386-8347-7/22/$31.00 ©2022 IEEE | DOI: 10.1109/ICC45855.2022.9838399

***Abstract*—We consider a relay-aided massive multi-input multi-output (mMIMO) system where a base station (BS) serves various users via multiple relays by employing non-orthogonal multiple access (NOMA). We practically model this system by considering spatially-correlated Rician-faded channels, and channel estimation errors both at the BS and at the users, which consequently perform imperfect successive interference cancellation (SIC). We consider these two artifacts, and derive a lower bound on the spectral efficiency (SE) of this multi-relay NOMA system, which is valid for arbitrary number of BS antennas. We crucially show that i) Rician-faded channels are immune to the errors caused by imperfect SIC at users; ii) high spatial correlation improves the spatial diversity among relays located close to BS and achieves better sum SE than its uncorrelated counterpart.**

I. Introduction

Non-orthogonal multiple access (NOMA), which multiplexes users in the power domain, is shown to have a higher spectral efficiency (SE) than orthogonal multiple access (OMA) [1], [2]. Users in a NOMA system mitigate multi-user interference by employing successive interference cancellation (SIC) at the receiver. Massive multi-input multi-output (mMIMO) technology, where in a base station (BS) equipped with massive antennas arrays, leverages spatial diversity to serve multiple users on the same spectral resource, offers large SE and energy efficiency gains [3], [4]. Integrating NOMA with a mMIMO system can significantly boost the system SE, and is recently investigated in [1], [2]. Reference [1] analyzed the outage probability and ergodic rate of a downlink mMIMO NOMA system with imperfect SIC. Reference [2] proposed various user-clustering and pilot assignment strategies for a NOMA-aided downlink multi-cell mMIMO system.

Relay assisted mMIMO NOMA systems, wherein the BS serves various users via relays, further improves the SE along with the coverage. These systems have recently been analyzed in [5], [6]. Reference [5] derived a closed form SE expression for a multi-relay mMIMO NOMA system with zero forcing (ZF) precoding at the BS. This work assumed perfect channel state information (CSI) at the BS, and perfect SIC at the users. Mandawaria *et al.* [6] extended the work in [5] and derived closed-form SE expressions by considering CSI errors at the BS and imperfect SIC at the users. Both these works assumed *uncorrelated Rayleigh faded channels*.

A mMIMO BS, due to its closely spaced antennas and lack of rich scattering environment, experiences *spatially-correlated* channels [2], [7]. Further, due to the proximity of users, relays and BS, *the channels have a deterministic line of sight (LoS) components* [7], [8], which the existing works have ignored. Reference [7] considered a spatially-correlated relay-enabled mMIMO NOMA system with MR processing at the BS. This work, however, ignored the LoS components in the channels and derived approximate SE expression. Zhang *et al.* in [8] analyzed the SE of a *single-hop* downlink cell-free mMIMO NOMA system with spatially-correlated Rician faded channels. This work however did not consider relays in its system. Both spatial correlation and LoS components are vital aspects which can impact the gains accrued by relays, mMIMO and NOMA. The current work addresses these gaps with its **main contributions** listed below.

1) We consider a multi-relay aided mMIMO NOMA system with spatially-correlated Rician-faded channels. The BS and the users, unlike [5], do not have the CSI knowledge, and therefore estimate the same, by using the pilots transmitted by the relays. We address the derivation difficulty caused by the imperfect SIC/CSI and the spatially-correlated Rician channels, and derive the closed-form SE lower bound which is a function of long-term channel statistics. The *spatially-correlated Rician-faded channels* considerably complicates the SE analysis when compared with [6], [7], which consider *uncorrelated Rayleigh-faded* channels.
2) We numerically validate the derived closed-form SE lower bound and draw insights which can help in designing practical systems. For example, we show that a Rician-faded system has higher immunity to the imperfect SIC when compared with its Rayleigh counterpart. Further, correlation increases the spatial diversity among relays, specifically when they are close to BS, and leads to a higher sum-SE than the uncorrelated case.

II. System Model

We consider a cellular system where an N-antenna mMIMO BS wants to serve K_u cell-edge users who, due to high path loss, have a extremely weak direct link with the BS. The BS serves such users via K single-antenna half-duplex amplify-and-forward (AF) relays, which are simple to implement. They are installed such that the BS-relay and relay-user channels have a strong LoS component along with the non LoS (NLoS) one. This implies that these channels have Rician probability density function (pdf). The BS communicates with a cluster of U_k single-antenna users on the same spectral resource by employing NOMA via the kth relay.[1] A coherence interval of τ_c symbols is split into channel estimation (CE) and data transmission phases of $\tau \leq \tau_c$ and $(\tau_c - \tau)$ symbols, respectively. Before explaining the signal model of CE and data transmission phases, we briefly model different channels in the system.

[1]We assume $k = 1, \cdots, K$ and $n = 1, \cdots, U_k$ throughout this paper.

Channel model: The spatially-correlated Rician-faded channel from the BS to kth relay, denoted as $\mathbf{h}_k \in \mathbb{C}^{N\times 1}$ is modeled as

$$\mathbf{h}_k = \sqrt{\frac{K_{h_k}\beta_{h_k}}{1+K_{h_k}}}\mathbf{h}_k^{\text{LoS}} + \sqrt{\frac{\beta_{h_k}}{1+K_{h_k}}}\overline{\mathbf{R}}_{h_k}^{\frac{1}{2}}\mathbf{h}_k^{\text{NLoS}}. \quad (1)$$

Here K_{h_k} is the Rician factor, and β_{h_k} is the large-scale fading coefficient. The vectors $\mathbf{h}_k^{\text{NLoS}} \sim \mathcal{CN}(0, \mathbf{I}_N)$ and $\mathbf{h}_k^{\text{LoS}} = \left[1, e^{j2\pi d_{h_k}\sin(\varphi_{h_k})}, \ldots, e^{j2\pi d_{h_k}(N-1)\sin(\varphi_{h_k})}\right]^T$ model the NLoS and LoS components, respectively. Here φ_{h_k} is the nominal angle between the BS and kth relay, and d_{h_k} is the inter-antenna distance. The matrix $\overline{\mathbf{R}}_{h_k}$ characterizes the spatial correlation of the NLoS component.

The channel vector from the k'th relay to the nth user in kth cluster is denoted as $g_{k',k,n} \in \mathbb{C}^{1\times 1}$ and is modeled as

$$g_{k',k,n} = \sqrt{\frac{K_{g_{k',k,n}}\beta_{g_{k',k,n}}}{1+K_{g_{k',k,n}}}} + \sqrt{\frac{\beta_{g_{k',k,n}}}{1+K_{g_{k',k,n}}}}g_{k',k,n}^{\text{NLoS}}. \quad (2)$$

Here $K_{g_{k',k,n}}$ is the Rician factor and $\beta_{g_{k',k,n}}$ is the large-scale fading coefficient. The scalar $g_{k',k,n}^{\text{NLoS}} \sim \mathcal{CN}(0,1)$ model the small-scale fading in the NLoS component.

Channel Estimation: During this phase, the kth relay transmits $\tau \geq K$-length mutually orthogonal pilot $\boldsymbol{\psi}_k$ to the BS and users. The BS uses this pilot to estimate $\mathbf{h}_k$ i.e., its first-hop uplink CSI from the kth relay. The nth user associated with the kth relay uses the same pilot to estimate $g_{k,k,n}$ i.e., its second-hop downlink CSI from the kth relay. The pilot signal received by the BS and by the nth user associated with kth relay are respectively given as follows:

$$\mathbf{Y}^{\text{BP}} = \sqrt{\tau p_p}\sum_{k=1}^{K}\mathbf{h}_k\boldsymbol{\psi}_k^H + \mathbf{N}^{\text{BP}} \text{ and}$$

$$\mathbf{y}_{k,n}^p = \sqrt{\tau p_p}\sum_{k'=1}^{K} g_{k,k,n}\boldsymbol{\psi}_{k'}^H + \mathbf{n}_{k,n}^p. \quad (3)$$

Here p_p is the pilot transmit power and $\mathbf{N}^{\text{BP}} \in \mathbb{C}^{N\times\tau}$ (resp. $\mathbf{n}_{k,n}^p$) is the additive white Gaussian noise (AWGN) at the BS (resp. user) with independent and identically distributed (i.i.d) $\mathcal{CN}(0,1)$ elements. The BS estimates $\mathbf{h}_k$ by projecting $\mathbf{Y}^{\text{BP}}$ on to $\boldsymbol{\psi}_k$ as $\tilde{\mathbf{y}}_k^{\text{BP}} = \mathbf{Y}^{\text{BP}}\boldsymbol{\psi}_k = \sqrt{\tau p_p}\mathbf{h}_k + \mathbf{N}^{\text{BP}}\boldsymbol{\psi}_k$. The MMSE estimate of channel $\mathbf{h}_k$ is obtained using $\tilde{\mathbf{y}}_k^{\text{BP}}$ as

$$\hat{\mathbf{h}}_k = \overline{\mathbf{h}}_k + \sqrt{\tau p_p}\mathbf{R}_{h_k}\boldsymbol{\Psi}_{h_k}\left[\tilde{\mathbf{y}}_k^{\text{BP}} - \mathbb{E}\left(\overline{\mathbf{y}}_k^{\text{BP}}\right)\right], \quad (4)$$

where $\boldsymbol{\Psi}_{h_k} = \left(\mathbf{I} + \tau p_p\mathbf{R}_{h_k}\right)^{-1}$ with $\mathbf{R}_{h_k} = \frac{\beta_{h_k}}{1+K_{h_k}}\overline{\mathbf{R}}_{h_k}$ and $\bar{\mathbf{y}}_k^{\text{BP}} = \sqrt{\tau p_p}\bar{\mathbf{h}}_k$. The channel estimation error $\boldsymbol{\varepsilon}_k = \mathbf{h}_k - \hat{\mathbf{h}}_k$ is distributed as $\boldsymbol{\varepsilon}_k \sim \mathcal{CN}(0, \mathbf{R}_{h_k} - \tau p_p\mathbf{R}_{h_k}\boldsymbol{\Psi}_{h_k}\mathbf{R}_{h_k})$ [9].

To estimate $g_{k,k,n}$, the nth user associated with the kth relay, similar to the BS, projects its received signal $\mathbf{y}_{k,n}^p$ onto $\boldsymbol{\psi}_k$ as $\tilde{y}_{k,k,n}^{\text{P}} = \mathbf{y}_{k,n}^p\boldsymbol{\psi}_k = \sqrt{\tau p_p}g_{k,k,n} + \mathbf{n}_{k,n}^{\text{RP}}\boldsymbol{\psi}_k$. The MMSE estimate of $g_{k,k,n}$ is [9]

$$\hat{g}_{k,k,n} = \overline{g}_{k,k,n} + \frac{\sqrt{\tau p_p}\gamma_{g_{k,k,n}}}{1+\tau p_p\gamma_{g_{k,k,n}}}\left[\tilde{y}_{k,k,n}^{\text{P}} - \overline{y}_{k,k,n}^{\text{P}}\right], \quad (5)$$

where $\overline{y}_{k,k,n} = \sqrt{\tau p_p}\overline{g}_{k,k,n}$ and $\gamma_{g_{k,k,n}} = \frac{\beta_{g_{k,k,n}}}{(1+K_{g_{k,k,n}})}$. Similarly, the estimation error $e_{k,k,n} = g_{k,k,n} - \hat{g}_{k,k,n}$ is distributed as $e_{k,k,n} \sim \mathcal{CN}\left(0, \gamma_{k,k,n} - \frac{\tau p_p\gamma_{g_{k,k,n}}^2}{\tau p_p\gamma_{g_{k,k,n}}+1}\right)$ [9].

Data transmission: The data transmission from BS to user occurs in two slots. In the first slot, the BS uses NOMA to superpose transmit signals of different users, precodes it and transmits to the relays. Let $s_{k,n}$ be the signal of the nth user in kth cluster. The precoded NOMA signal transmitted by the BS is accordingly given as follows:

$$\mathbf{x}_b = \sum_{k=1}^{K}\mathbf{w}_k\sum_{n=1}^{U_k}\sqrt{p_{k,n}}s_{k,n} \triangleq \sum_{k=1}^{K}\mathbf{w}_k x_k. \quad (7)$$

Here $x_k = \sum_{n=1}^{U_k}\sqrt{p_{k,n}}s_{k,n}$ is the NOMA signal for the kth relay, $\mathbf{w}_k \in \mathbb{C}^{N\times 1}$ is the transmit precoder and $p_{k,n}$ is the transmit power of the nth user associated with the kth relay, respectively. The precoder $\mathbf{w}_k$ is designed based on MRC principles as $\mathbf{w}_k = \hat{\mathbf{h}}_k^* \Big/ \sqrt{\mathbb{E}\left(\left\|\hat{\mathbf{h}}_k\right\|^2\right)}$ [7], [10]. The signal received by the kth relay is given as

$$y_{R_k} = \sum_{k'=1}^{K}\mathbf{h}_k^T\mathbf{w}_{k'}x_{k'} + z_{R_k}, \quad (8)$$

Here the scalar $z_{R_k} \sim \mathcal{CN}(0,1)$ is the AWGN at the kth relay.

In the second slot, the kth AF relay amplifies its received precoded NOMA signal as $x_{R_k} = \mu_k y_{R_k}$, and then broadcasts it to the users in its cluster. Here μ_k is the amplification factor designed to constrain the maximum relay transmit power to q_k i.e., $\mathbb{E}[|x_{R_k}|^2] = q_k$. The expression for amplification factor is therefore given as

$$\mu_k = \sqrt{\frac{q_k}{\mathbb{E}\Big[\Big|\sum_{k'=1}^{K}\mathbf{h}_k^T\mathbf{w}_{k'}x_{k'}\Big|^2\Big] + \mathbb{E}\left[|z_{R,k}|^2\right]}}. \quad (9)$$

The transmit signal of the K relays interfere with each other and the nth user in the kth cluster receives a sum-signal $\hat{y}_{k,n} = \sum_{k'=1}^{K}g_{k',k,n}x_{R_{k'}} + z_{k,n}$, where $z_{k,n}$ is the AWGN at the nth user associated with the kth relay. The user $S_{k,n}$, using the estimated CSI $\hat{g}_{k,k,n}$, equalizes its received signal as

$$y_{k,n} = f_{k,n}\hat{y}_{k,n} = f_{k,n}\left(\sum_{k'=1}^{K}g_{k',k,n}x_{R_{k'}} + z_{k,n}\right). \quad (10)$$

Here the equalizer $f_{k,n}$ is designed as $f_{k,n} = \hat{g}_{k,k,n}^*/|\hat{g}_{k,k,n}|$, where $\hat{g}_{k,k,n}$ is the MMSE estimate of channel $g_{k,k,n}$ [6]. The equalized user signal $y_{k,n}$, by substituting $x_{R_{k'}} = \mu_{k'}y_{R_{k'}}$ and using (8), is re-expressed in (11) shown at the top of next page.

In (11), the intra-relay interference is caused by the data signals corresponding to other users served by the kth relay, the 2nd hop inter-relay interference is caused by the amplified transmit signal of other relays that are serving their respective user clusters. The 1st hop inter-relay interference is because the BS precodes NOMA signals of multiple relays using MR precoding, and the kth relay amplifies the NOMA signal intended for other relays.

Imperfect SIC at the user: In a NOMA system, users served by the kth relay mitigate their intra-relay interference by using SIC. To achieve this, without loss of generality, we assume that the users served by kth relay are ordered in the descending order of their channel statistics [7]. The nth user

$$y_{k,n} = \underbrace{f_{k,n}g_{k,k,n}\mu_k\mathbf{h}_k^T\mathbf{w}_k\sqrt{p_{k,n}}s_{k,n}}_{\text{desired signal}} + \underbrace{f_{k,n}g_{k,k,n}\mu_k\mathbf{h}_k^T\mathbf{w}_k\sum_{n'=1,n'\neq n}^{U_k}\sqrt{p_{k,n'}}s_{k,n'}}_{\text{intra-relay interference}} + \underbrace{\sum_{k'\neq k}^{K}\sum_{n'=1}^{U_{k'}} f_{k,n}g_{k',k,n}\mu_{k'}\mathbf{h}_{k'}^T\mathbf{w}_{k'}\sqrt{p_{k',n'}}s_{k',n'}}_{\text{inter-relay interference at 2nd hop}}$$
$$+ \underbrace{\sum_{k'=1}^{K}\sum_{k''\neq k'}^{K}\sum_{n'=1}^{U_{k''}} f_{k,n}g_{k',k,n}\mu_{k'}\mathbf{h}_{k'}^T\mathbf{w}_{k''}\sqrt{p_{k'',n'}}s_{k'',n'}}_{\text{inter-relay interference at 1st hop}} + \underbrace{\sum_{k'=1}^{K} f_{k,n}g_{k',k,n}\mu_{k'}z_{R,k'}}_{\text{forwarding noise}} + \underbrace{f_{k,n}z_{k,n}}_{\text{receiver noise}}. \quad (11)$$

$$\bar{y}_{k,n} = f_{k,n}g_{k,k,n}\mu_k\mathbf{h}_k^T\mathbf{w}_k\sqrt{p_{k,n}}s_{k,n} + \sum_{k'\neq k}^{K}\sum_{n'=1}^{U_{k'}} f_{k,n}g_{k;k,n}\mu_{k'}\mathbf{h}_{k'}^T\mathbf{w}_{k'}\sqrt{p_{k;n'}}s_{k;n'}$$
$$+ \underbrace{f_{k,n}g_{k,k,n}\mu_k\mathbf{h}_k^T\mathbf{w}_k\sum_{n'=1}^{n-1}\sqrt{p_{k,n'}}s_{k,n'}}_{\text{inherent intra-relay interference}} + \underbrace{\sum_{n'=n+1}^{U_k}\mu_k\left[f_{k,n}g_{k,k,n}\mathbf{h}_k^T\mathbf{w}_k - f_{k,n}\hat{g}_{k,k,n}\mathbb{E}\left[\mathbf{h}_k^T\mathbf{w}_k\right]\right]\sqrt{p_{k,n'}}s_{k,n'}}_{\text{residual intra-relay interference}}$$
$$+ \sum_{k'=1}^{K}\sum_{k''\neq k}^{K}\sum_{n'=1}^{U_{k''}} f_{k,n}g_{k',k,n}\mu_{k'}\mathbf{h}_{k'}^T\mathbf{w}_{k''}\sqrt{p_{k'',n'}}s_{k'',n'} + \sum_{k'=1}^{K} f_{k,n}g_{k',k,n}\mu_{k'}z_{R,k'} + f_{k,n}z_{k,n}. \quad (12)$$

associated with kth relay first cancels intra-relay interference from $\forall\, n' > n$ users by employing SIC [7], and then decodes its own signal while treating the signal from the first $n-1$ users as inherent intra-cluster interference [6], [7]. We similar to [6] assume that the user employs statistical value $\mathbb{E}[\mathbf{h}_k^T\mathbf{w}_k]$ and its channel estimate $\hat{g}_{k,k,n}$ to perform SIC. The post-SIC receive signal at the nth user associated with the kth relay, denoted as $\bar{y}_{k,n}$, is given in (12) shown at the top of the page.

III. Achievable SE analysis

In this section, we employ hardening bound technique [10], to derive a closed-form SE lower bound by considering imperfect CSI and imperfect SIC at the BS and users, respectively. Using this technique, we split the the user receive signal in (12) into signal received over *hardened* channel $\mathbb{E}[\mu_k f_{k,n}g_{k,k,n}\mathbf{h}_k^T\mathbf{w}_k]$ plus effective noise as shown below

$$\bar{y}_{k,n} = \underbrace{\mu_k\mathbb{E}\left[f_{k,n}g_{k,k,n}\mathbf{h}_k^T\mathbf{w}_k\right]\sqrt{p_{k,n}}s_{k,n}}_{\text{true desired signal}} + \bar{z}_{k,n}, \text{ where } (13)$$

$$\bar{z}_{k,n} = \underbrace{\mu_k\left(f_{k,n}g_{k,k,n}\mathbf{h}_k^T\mathbf{w}_k - \mathbb{E}\left[f_{k,n}g_{k,k,n}\mathbf{h}_k^T\mathbf{w}_k\right]\right)\sqrt{p_{k,n}}s_{k,n}}_{\text{beamforming uncertainty}}$$
$$+ f_{k,n}g_{k,k,n}\mu_k\mathbf{h}_k^T\mathbf{w}_k\sum_{n'=1}^{n-1}\sqrt{p_{k,n'}}s_{k,n'}$$
$$+ \sum_{n'=n+1}^{U_k}\mu_k\left[f_{k,n}g_{k,k,n}\mathbf{h}_k^T\mathbf{w}_k - f_{k,n}\hat{g}_{k,k,n}\mathbb{E}\left[\mathbf{h}_k^T\mathbf{w}_k\right]\right]\sqrt{p_{k,n'}}s_{k,n'}$$
$$+ \sum_{k'\neq k}^{K}\sum_{n'=1}^{U_{k'}} f_{k,n}g_{k;k,n}\mu_{k'}\mathbf{h}_{k'}^T\mathbf{w}_{k'}\sqrt{p_{k;n'}}s_{k;n'}$$
$$+ \sum_{k'=1}^{K}\sum_{k''\neq k'}^{K}\sum_{n'=1}^{U_{k''}} f_{k,n}g_{k',k,n}\mu_{k'}\mathbf{h}_{k'}^T\mathbf{w}_{k''}\sqrt{p_{k'',n'}}s_{k'',n'}$$
$$+ \sum_{k'=1}^{K} f_{k,n}g_{k',k,n}\mu_{k'}z_{R,k'} + f_{k,n}z_{k,n}. \quad (14)$$

It is easy to confirm that the true desired signal in (13) is uncorrelated with the effective noise $\bar{z}_{k,n}$. Further, similar to [2], [10], we use central limit theorem to treat the effective noise $\bar{z}_{k,n}$ as a worst case Gaussian noise. The resultant lower bound on the achievable sum SE is given as

$$\overline{R}_{\text{sum}} = \frac{1}{2}\left(1-\frac{\tau}{\tau_c}\right)\sum_{k=1}^{K}\sum_{n=1}^{U_k}\left[\log_2\left(1+\frac{\overline{\Delta}_{k,n}}{\overline{\Omega}_{k,n}}\right)\right], \text{ where } (15)$$

$$\overline{\Delta}_{k,n} = \left|\mathbb{E}\left[f_{k,n}g_{k,k,n}\mathbf{h}_k^T\mathbf{w}_k\right]\right|^2 p_{k,n},\ \overline{\Omega}_{k,n} = \sum_{l=1}^{5}\overline{I}_{k,n}^{(l)},$$
$$\overline{I}_{k,n}^{(0)} = \mathbb{E}\left[\left|\mu_k\left(f_{k,n}g_{k,k,n}\mathbf{h}_k^T\mathbf{w}_k - \mathbb{E}\left[f_{k,n}g_{k,k,n}\mathbf{h}_k^T\mathbf{w}_k\right]\right)\right|^2\right]p_{k,n},$$
$$\overline{I}_{k,n}^{(1)} = \mathbb{E}\left[\left|f_{k,n}g_{k,k,n}\mu_k\mathbf{h}_k^T\mathbf{w}_k\right|^2\right]\sum_{n'=1}^{n-1}p_{k,n'},$$
$$\overline{I}_{k,n}^{(2)} = \sum_{n'=n+1}^{U_k}\mathbb{E}\left[\left|f_{k,n}g_{k,k,n}\mathbf{h}_k^T\mathbf{w}_k - f_{k,n}\hat{g}_{k,k,n}\mathbb{E}\left[\mathbf{h}_k^T\mathbf{w}_k\right]\right|^2\right]\mu_k^2 p_{k,n'}$$
$$\overline{I}_{k,n}^{(3)} = \sum_{k'\neq k}^{K}\sum_{n'=1}^{U_{k'}}\mathbb{E}\left[\left|f_{k,n}g_{k',k,n}\mu_{k'}\mathbf{h}_{k'}^T\mathbf{w}_{k'}\right|^2\right]p_{k',n'},$$
$$\overline{I}_{k,n}^{(4)} = \sum_{k'=1}^{K}\sum_{k''\neq k'}^{K}\sum_{n'=1}^{U_{k''}}\mathbb{E}\left[\left|f_{k,n}g_{k',k,n}\mu_{k'}\mathbf{h}_{k'}^T\mathbf{w}_{k''}\right|^2\right]p_{k'',n'},$$
$$\text{and } \overline{I}_{k,n}^{(5)} = \sum_{k'=1}^{K}\mathbb{E}\left[\left|f_{k,n}g_{k',k,n}\mu_{k'}\right|^2\right]. \quad (16)$$

Here $\overline{I}_{k,n}^{(0)},\cdots,\overline{I}_{k,n}^{(5)}$ are the power of the beamforming uncertainty, inherent intra-relay interference, residual intra-relay interference, 2nd hop inter-relay interference, 1st hop inter-relay interference and amplified relay noise, respectively. We next calculate the expectations in (16) to obtain a closed form SE expression. The spatially-correlated Rician faded-channels and imperfect CSI/SIC at BS and users, considerably complicate these calculations when compared with [6], [7].

Theorem 1. The closed form SE of the nth user in the kth relay for a finite number of BS antennas relying on MMSE channel estimation, and with imperfect user SIC, is obtained as

$$\widetilde{R}_{k,n} = \frac{1}{2}\left(1-\frac{\tau}{\tau_c}\right)\log_2\left(1+\frac{\widetilde{P}_{k,n}}{\sum_{l=1}^{5}\widetilde{I}_{k,n}^{(l)}+1}\right), \text{ where } (17)$$

$$\widetilde{P}_{k,n} = A_{k,n}\tilde{\mu}_k^2 p_{k,n}, \qquad \tilde{I}_{k,n}^{(0)} = C_{k,n}^{(0)} p_{k,n}\tilde{\mu}_k^2,$$

$$\tilde{I}_{k,n}^{(1)} = C_{k,n}^{(1)} \sum_{n'=1}^{n-1} \tilde{\mu}_k^2 p_{k,n'}, \qquad \tilde{I}_{k,n}^{(2)} = C_{k,n}^{(2)} \sum_{n'=n+1}^{U_k} p_{k,n'}\tilde{\mu}_k^2,$$

$$\tilde{I}_{k,n}^{(3)} = \sum_{k'\neq k}^{K} \sum_{n'=1}^{U_{k'}} C_{k',k,n}^{(3)} p_{k',n'}\mu_{k'}^2, \quad \tilde{\mu}_k = \frac{q_k}{\left(\xi_{kk}p_k + \sum_{j=1}^{K}\rho_{kj}p_j + 1\right)},$$

$$\tilde{I}_{k,n}^{(4)} = \sum_{k'=1}^{K} \sum_{k''\neq k'}^{K} \sum_{n'=1}^{U_{k''}} C_{k',k'',n'}^{(4)} p_{k'',n'}\tilde{\mu}_{k'}^2, \; p_k = \sum_{n=1}^{U_k} p_{k,n} \text{ and}$$

$$\tilde{I}_{k,n}^{(5)} = \sum_{k'=1}^{K} \left(\left|\bar{g}_{k',k,n}\right|^2 + \gamma_{g_{k',k,n}}\right)\tilde{\mu}_{k'}^2.$$

The constants $A_{k,n}$, $C_{k,n}^{(0)}$, $C_{k,n}^{(1)}$, $C_{k,n}^{(2)}$, $C_{k',k,n}^{(3)}$ and $C_{k,n}^{(4)}$ are functions of long term channel statistics and are given in Appendix A

Asymptotic SE expression: We now use the derived lower-bound to derive asymptotic SE result when the rician factors $\{K_{h_k}\}_{\forall k} = K_h$, $\{K_{g_{k,k',n}}\}_{\forall k,k',n} = K_g$ and BS antennas N jointly tend to infinity. The term $\widetilde{P}_{k,n}^{(0)}$ in Theorem 1, as $(K_h, K_g, N) \to \infty$, simplifies to

$$\overline{P}_{k,n}^{(0)} = \frac{\pi \upsilon_{k,k,n}\delta_k}{4} L_{k,n}^2 \frac{q_k p_{k,n}}{\xi_{kk}p_k + \sum_{j=1}^{K}\rho_{kj}p_j + 1} \overset{(a)}{=} \frac{p_{k,n}q_k}{p_k}\beta_{g_{k,k,n}}.$$

Here equality (a) is obtained by substituting $\bar{\mathbf{h}}_k = \sqrt{\beta_{h_k}}\mathbf{h}_k^{\text{LoS}}$, $\bar{g}_{k,k',n} = \sqrt{\beta_{g_{k,k',n}}}$, $\overline{\mathbf{R}}_{h_k} = \mathbf{0}$ and using i) the result $\bar{\mathbf{h}}_k^H \bar{\mathbf{h}}_{k'} = N$, if $k' = k$ and ; $= 0$, otherwise; ii) the upper limit on Laguerre polynomial $L_{k,n} \xrightarrow{K_g \to \infty} \frac{|\bar{g}_{k,k',n}|^2}{\upsilon_{k,k,n}} \frac{4}{\pi}$ [11, 13.5.1]. The other terms in Theorem 1, on similar lines, can be calculated as $\tilde{I}_{k,n}^{(0)} \to 0$, $\tilde{I}_{k,n}^{(1)} \to \beta_{g_{k,k,n}} \sum_{n'=1}^{n-1} \frac{p_{k,n'}q_k}{p_k}$, $\tilde{I}_{k,n}^{(2)} \to 0$, $\tilde{I}_{k,n}^{(3)} \to \sum_{k'\neq k}^{K} \beta_{g_{k',k,n}} q_{k'}$, $\tilde{I}_{k,n}^{(4)} \to 0$ and $\tilde{I}_{k,n}^{(5)} \to 0$. The final asymtotic SE expression is therefore given as

$$\overline{R}_{k,n}^{\infty} = \frac{(\tau_c - \tau)}{2\tau_c} \log_2\left(1 + \frac{\frac{p_{k,n}q_k}{p_k}\beta_{g_{k,k,n}}}{\beta_{g_{k,k,n}} \sum_{n'=1}^{n-1} \frac{q_k p_{k,n'}}{p_k} + \sum_{k'\neq k}^{K} \beta_{g_{k,k',n}} q_{k'} + 1}\right) \tag{18}$$

Asymptotic insights: We infer that as (K_h, K_g, N) tend to ∞,

- power of signal leakage $\overline{I}_{k,n}^{(0)}$ and of first-hop inter-relay interference $\overline{I}_{k,n}^{(4)}$ vanish. This is because the Rician factor and massive antennas together increase the channel hardening and favorable propagation properties of mMIMO system
- residual intra relay interference $\overline{I}_{k,n}^{(2)}$ goes to 0, which suggests that Rician factor and BS antennas, together reduces the effect of CSI/SIC errors on the system SE.
- SE in (18) i) is independent of the BS antennas N, and relay to BS channel large-scale coefficients; and ii) depends only on relay-user channel strengths. With increase in M, the SE therefore saturates to a non-zero finite value in (18).

IV. Simulation results

We now numerically corroborate the accuracy of the derived closed-form SE expression and assess the impact of spatial-correlation, Rician channels and imperfect SIC on the SE of multiple-relay-aided mMIMO NOMA system. We consider a practical multi-relay mMIMO system, wherein a mMIMO BS with $N = 100$ antennas is located at the centre of the cell and $K = 5$ relays are uniformly deployed at a distance of $R_r = 200$m from the BS. The $U_k = 5$ users in each cluster are randomly located within a circle of radius $R_u = 100$m around the relay. The large-scale fading coefficients of different channels in the system are as in [4, Eq. (68)]. The Rician factors $K_{h_k}, K_{g_{k,k',n}}$ are modeled as $K_{h_k}[\text{dB}] = 13 - 0.03d_{h_k}$ and $K_{g_{k',k,n}}[\text{dB}] = 13 - 0.03d_{g_{k',k,n}}$, respectively. Here d_{h_k} (resp. $d_{g_{k',k,n}}$) denotes the separation distance between kth user and BS (resp. nth user in kth cluster and k'th relay). The correlation matrices $\overline{\mathbf{R}}_{h_k}$ are modeled using Gaussian local scattering model with angular standard deviation (ASD) of 10°. We assume the bandwidth of $B = 20$ MHz, the relay pilot power as $p_p = 30$ dBm and relay power of $Q_T = 25$ dBm. The coherence interval has $\tau_c = 200$ symbols with a training period of $\tau = K = 5$ symbols. The system parameters remains fixed unless explicitly mentioned.

*1) **Validation of closed-form SE expression**:* We now show the accuracy of the derived closed-form SE expression. We plot in Fig. 1a sum SE versus BS transmit power P and compare the closed-form SE expression in Theorem 1 with its simulated SE counterpart in (15). For this study, we allocate equal power to all the user-data streams and relays i.e., $p_{k,n} = P_T/K_u$ and $q_k = Q_T \; \forall \; k = 1, \cdots, K$ and $n = 1, \cdots, U_k$. For different K values, we note that the closed-form curve exactly matches with the simulated, which validates the correctness of the derived closed-form expression. With increase in K, the sum SE initially increases, reaches its maximum at $K = 5$, and then decreases for $K = 10$. This is explained as follows

– For $K = 2$ relays, the relays are far apart and each relay serves $U_k = 10$ users. The users served by each relay therefore experience stronger intra relay interference (residual + inherent), which dominates over the inter-relay interference (1st hop + 2nd hop).
– With increase in number of relays from $K = 2$ to $K = 5$ i) the intra-relay interference reduces as each relay now serves less number of users and; ii) the inter-relay interference increases as the separation distance between the relays decreases. For $K = 5$, both inter-relay and intra-relay interferences are balanced and also minimum, which increases the sum SE.
– For $K \geq 5$, the separation distance between the relays is the least, and the inter-relay interference dominates over intra-relay, which reduces the sum SE values.

We further note that with increase in the BS transmit power P_T, the sum SE increases and then saturates for $P_T \geq 10$ dBm. This is because the users experience high inter-relay and intra-relay interferences at high BS transmit power. *This study reveals the optimal number of relays and relay-user ratio required to achieve optimal system sum SE.*

*2) **Impact of CSI errors and imperfect SIC**:* We next plot in Fig. 1b, sum SE versus number of BS antennas N using imperfect SIC for Rayleigh and Rician faded channels and compare it with the sum SE of perfect SIC case. For this study, we consider the following pilot powers $p_p = \{10, 30\}$ dBm.

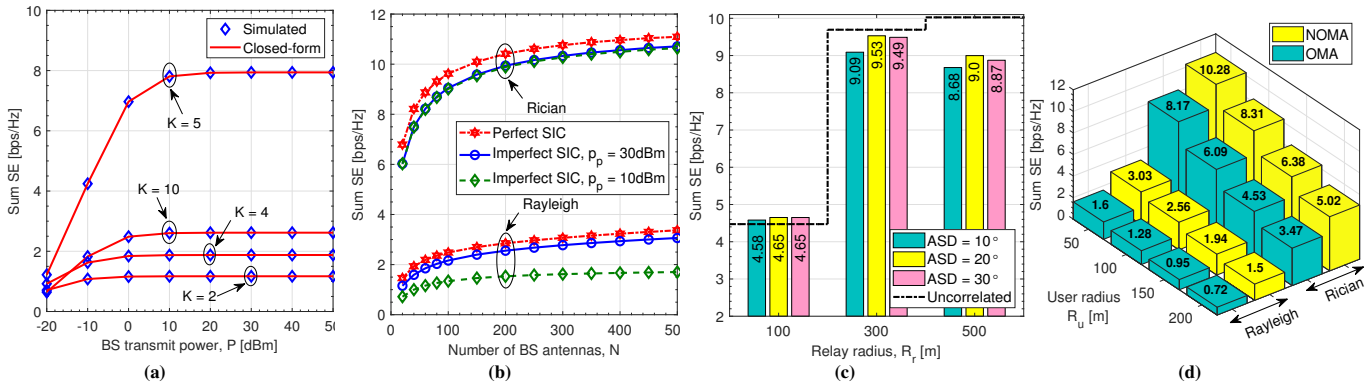

Fig. 1: a) sum SE versus BS transmit power; b) sum SE versus BS antennas N and c) sum SE versus R_r and; d) NOMA vs OMA comparison.

The sum SE for Rayleigh-faded channels is obtained by setting the Rician K factors $\{K_{h_k}, K_{g_{k',k,n}}\} = 0$ and by modelling the large scale fading coefficients as in [4, Eq. (69)]. The sum SE for perfect SIC is obtained by setting residual intra-relay interference to 0 in Theorem 1 i.e., $\tilde{I}^{(2)}_{k,n} = 0$. We first see that the Rician channel has a much higher SE. This is due to its LoS component which increases the channel gain. We also note that reducing the pilot power from $p_p = 30$ dBm to $p_p = 10$ dBm does not affect the sum SE of Rician channel, but considerably reduces the SE for the Rayleigh channel. This is because the MMSE channel estimator exploits the known LoS Rician components and improves the channel estimation performance, an aspect which becomes conspicuous at low pilot power. For Rayleigh faded channels without LoS link, the channel estimation consequently degrades. For NOMA, it is crucial to have good channel estimates as they help in increasing the quality of SIC [2]. *This study therefore crucially characterizes the pilot power behavior for mMIMO NOMA Rician/Rayleigh faded systems, an aspect which was not discussed in our earlier work in [6].*

3) ***Impact of spatial correlation and Rician factor****:* We now *compare in Fig. 1c the sum SE of spatially-correlated mMIMO NOMA system with that of an uncorrelated system (denoted by dotted line) by varying the ASD.* We perform this study for three different values of relay radius R_r. We note that for a particular ASD, the sum SE increases when the relay radius R_r is increased from 100 to 300 m, but reduces for $R_r = 500$ m. This is because for $R_r = 100$ m, the relays are close not only to the BS but also to other relays. The presence of strong LoS links leads to strong inter-relay (both first- and second-hop) interference. With increase in R_r from 100 m to 300 m, the inter-relay and relay-BS separation distance increases, which reduces the LoS strength, and consequently the inter-relay interference. We note that the increased R_r also reduces the channel strength. The reduction in former however dominates the latter, which increases the sum SE. For $R_r \geq 300$ m, the reduction in latter dominates the former, which reduces the SE. We lastly note that for $R_r = 100$ m, the mMIMO NOMA system with spatially-correlated channels has marginally higher sum SE than the uncorrelated ones. This is because the spatially-correlated relays channels lie in non-overlapping eigen-spaces [3], [10], and therefore create lesser inter-relay interference.

4) ***NOMA - OMA comparison****:* We now quantify in Fig. 1d the NOMA SE gain over its OMA counterpart for both Rayleigh- and Rician-faded channels by varying the user radius R_u. In OMA, the coherence interval is split into K slots, and in each slot, the K relays simultaneously serve K users [6]. For this study, we set $R_r = 100$ m, ASD $= 10°$ and $K = 5$ relays, and $K_u = 20$ users. We infer from Fig. 1d that NOMA outperforms OMA for both Rayleigh- and Rician-faded channels. Specifically, for $R_u = 50$ m and Rician (resp. Rayleigh) channels, NOMA has $1.25\times$ (resp. $1.8\times$) higher sum SE than OMA. With increase in R_u, the sum SE for both Rician- and Rayleigh-faded channels decreases by 50%. With increase in R_u, intra-relay interference, large-scale fading coefficients and K factor reduce. The reduced intra relay interference is not able to compensate for the former two factors, which reduces the sum SE.

V. Conclusion

We derived a SE lower bound for a multi-relay-aided massive MIMO NOMA system with imperfect CSI and SIC. We numerically showed that i) a NOMA system with imperfect CSI and Rician-faded channels has similar SE as that of NOMA system with perfect SIC and lower pilot powers; and ii) high spatial correlation mitigates inter-relay interference, and results in higher sum SE when relays are close to the BS. We also characterized the number of users per relay, and the relay-BS separation distance, that improves the NOMA SE.

Appendix A

We now derive the closed-form SE expressions, by simplifying each of the expectations in (16). We start with the amplification factor μ_k in (9) and note that the second term in (9) can be calculated as $\mathbb{E}(|z_{R_k}|^2) = 1$. We now consider the first term in the denominator of (9) and simplify it as follows

$$\mathbb{E}\left[\left|\sum_{k'=1}^{K} \mathbf{h}_k^T \mathbf{w}_{k'} x_{k'}\right|^2\right] \overset{(a)}{=} \sum_{k'=1}^{K} p_{k'} \mathbb{E}\left[\mathbf{h}_k^T \mathbf{w}_{k'} \mathbf{w}_{k'}^H \mathbf{h}_k^*\right] \quad (19)$$

Equality (a) is because, due to the statistical independence of the data signals $\{s_{k,n}\}$, $\forall k, n$, the expectation $\mathbb{E}(x_{k'} x^*_{k''}) = 0$, for $k'' \neq k'$ and; $= \sum_{n'=1}^{U_k} p_{k'n'} \triangleq p_{k'}$, for $k'' = k'$. We now

simplify the expectation in (19) for $k'=k$ and $k'\neq k$ cases:
• for $k'\neq k$, the expectation in (19) is simplified as

$$\mathbb{E}\left[\mathbf{h}_k^T\mathbf{w}_{k'}\mathbf{w}_{k'}^H\mathbf{h}_k^*\right]=\frac{\mathbb{E}\left[\mathbf{h}_k^T\hat{\mathbf{h}}_{k'}^*\hat{\mathbf{h}}_{k'}^T\mathbf{h}_k^*\right]}{\mathbb{E}(\|\hat{\mathbf{h}}_{k'}\|^2)}$$
$$\overset{(a)}{=}\frac{\mathrm{Tr}\left((\bar{\mathbf{h}}_k\bar{\mathbf{h}}_k^H+\mathbf{R}_{h_k})(\bar{\mathbf{h}}_{k'}\bar{\mathbf{h}}_{k'}^H+\widehat{\mathbf{R}}_{h_{k'}})\right)}{\delta_{k'}}\triangleq\rho_{kk'}. \quad (20)$$

Here equality (a) is calculated by rewriting the expectation using $\mathrm{Tr}(\mathbf{AB})=\mathrm{Tr}(\mathbf{BA})$ and using $\mathbb{E}(\mathbf{h}_k^*\mathbf{h}_k^T)=[\bar{\mathbf{h}}_k\bar{\mathbf{h}}_k^H+\mathbf{R}_{h_k}]$ and $\mathbb{E}(\left\|\hat{\mathbf{h}}_{k'}\right\|^2)=\mathrm{Tr}(\bar{\mathbf{h}}_{k'}\bar{\mathbf{h}}_{k'}^H+\widehat{\mathbf{R}}_{h_{k'}})\triangleq\delta_{k'}$ with $\widehat{\mathbf{R}}_{h_k}=\tau p_p\mathbf{R}_{h_k}\boldsymbol{\Psi}_{h_k}^{-1}\mathbf{R}_{h_k}$.
• for $k'=k$, the expectation is simplified as

$$\mathbb{E}\left[\mathbf{h}_k^T\mathbf{w}_k\mathbf{w}_k^H\mathbf{h}_k^*\right]\overset{(a)}{=}\frac{\mathbb{E}\left[\hat{\mathbf{h}}_k^T\hat{\mathbf{h}}_k^*\hat{\mathbf{h}}_k^T\hat{\mathbf{h}}_k^*\right]}{\delta_k}+\frac{\mathbb{E}\left[\boldsymbol{\varepsilon}_k^T\hat{\mathbf{h}}_k^*\hat{\mathbf{h}}_k^T\boldsymbol{\varepsilon}_k^*\right]}{\delta_k}. \quad (21)$$

Equality (a) is obtained by i) substituting $\mathbf{h}_k=\hat{\mathbf{h}}_k+\boldsymbol{\varepsilon}_k$; ii) exploiting the statistical independence of MMSE estimate and estimation error and; iii) using $\mathbb{E}(\left\|\hat{\mathbf{h}}_k\right\|^2)=\delta_k$. The expectations $\mathbb{E}(\hat{\mathbf{h}}_k^T\hat{\mathbf{h}}_k\hat{\mathbf{h}}_k^H\hat{\mathbf{h}}_k^*)$ and $\mathbb{E}(\boldsymbol{\varepsilon}_k^T\hat{\mathbf{h}}_k^*\hat{\mathbf{h}}_k^T\boldsymbol{\varepsilon}_k^*)$ are obtained as

$$\mathbb{E}(\hat{\mathbf{h}}_k^T\hat{\mathbf{h}}_k^*\hat{\mathbf{h}}_k^T\hat{\mathbf{h}}_k^*)\overset{(a)}{=}\left|\mathrm{Tr}(\widehat{\mathbf{R}}_{h_k})\right|^2+\mathrm{Tr}(\widehat{\mathbf{R}}_{h_k}^2)+\left|\bar{\mathbf{h}}_k^H\bar{\mathbf{h}}_k\right|^2$$
$$+2\mathrm{Re}\left\{\mathrm{Tr}(\widehat{\mathbf{R}}_{h_k})\bar{\mathbf{h}}_k^H\bar{\mathbf{h}}_k+\bar{\mathbf{h}}_k^H\widehat{\mathbf{R}}_{h_k}\bar{\mathbf{h}}_k\right\}\text{ and} \quad (22)$$

$$\mathbb{E}(\boldsymbol{\varepsilon}_k^T\hat{\mathbf{h}}_k^*\hat{\mathbf{h}}_k^T\boldsymbol{\varepsilon}_k^*)=\mathrm{Tr}((\mathbf{R}_{h_k}-\widehat{\mathbf{R}}_{h_k})(\bar{\mathbf{h}}_k\bar{\mathbf{h}}_k^H+\widehat{\mathbf{R}}_{h_k})). \quad (23)$$

Equality (a) is obtained by using the fact that $\hat{\mathbf{h}}_k\sim\mathcal{CN}(\bar{\mathbf{h}}_k,\widehat{\mathbf{R}}_{h_k})$ and then using Lemma 5 from [4]. Equality (b) is obtained using the results $\mathbb{E}(\boldsymbol{\varepsilon}_k^*\boldsymbol{\varepsilon}_k^T)=\mathbf{R}_{h_k}-\widehat{\mathbf{R}}_{h_k}$ and $\mathbb{E}(\hat{\mathbf{h}}_k^*\hat{\mathbf{h}}_k^T)=\bar{\mathbf{h}}_k\bar{\mathbf{h}}_k^H+\widehat{\mathbf{R}}_{h_k}$. The closed-form expression of $\mathbb{E}(\mathbf{h}_k^T\mathbf{w}_k\mathbf{w}_k^H\mathbf{h}_k^*)$ is therefore obtained using (22) and (23) as

$$\mathbb{E}\left[\left|\mathbf{h}_k^T\mathbf{w}_k\right|^2\right]=(\rho_{kk}+\xi_{kk}), \quad (24)$$

where $\xi_{kk}=\frac{1}{\delta_k}\left[\left|\mathrm{Tr}\big(\widehat{\mathbf{R}}_{h_k}\big)\right|^2+2\mathrm{Re}\big\{\mathrm{Tr}\big(\widehat{\mathbf{R}}_{h_k}\big)\overline{\mathbf{h}}_k^H\overline{\mathbf{h}}_k\big\}\right]$. The closed-form expression for the amplification factor μ_k is therefore obtained clubbing (20) and (24) as

$$\tilde{\mu}_k=\sqrt{\frac{q_k}{\xi_{kk}p_k+\sum_{j=1}^K\rho_{kj}p_j+1}} \quad (25)$$

We now simplify the term $\overline{\Delta}_{k,n}$ in (16) as follows

$$\overline{\Delta}_{k,n}=\mu_k^2p_{k,n}\left|\mathbb{E}\left[\frac{\hat{g}_{k,k,n}}{|\hat{g}_{k,k,n}|}g_{k,k,n}\right]\right|^2\left|\mathbb{E}\left[\mathbf{h}_k^T\frac{\hat{\mathbf{h}}_k^*}{\sqrt{\mathbb{E}(\|\hat{\mathbf{h}}_k\|^2)}}\right]\right|^2$$
$$\overset{(a)}{=}\mu_k^2p_{k,n}|\mathbb{E}(|\hat{g}_{k,k,n}|)|^2\left|\sqrt{\mathbb{E}(\|\hat{\mathbf{h}}_k\|^2)}\right|^2$$
$$\overset{(b)}{=}\mu_k^2p_{k,n}\delta_k\frac{\pi}{4}\upsilon_{k,k,n}\left[L_{1/2}\left(\frac{-\left|\overline{g}_{k,k,n}\right|^2}{\upsilon_{k,k,n}}\right)\right]^2\triangleq A_{k,n}\tilde{\mu}_k^2p_{k,n}.$$

Here $A_{k,n}=\frac{\pi}{4}\delta_k\upsilon_{k,k,n}\left[L_{\frac{1}{2}}\left(\frac{-\left|\overline{g}_{k,k,n}\right|^2}{\upsilon_{k,k,n}}\right)\right]^2$ with $\upsilon_{k,k,n}=\frac{\tau p_p\gamma_{g_{k,k,n}}^2}{\tau p_p\gamma_{g_{k,k,n}}+1}$. Equality (a) is obtained by substituting $\mathbf{h}_k=\hat{\mathbf{h}}_k+\boldsymbol{\varepsilon}_k$, $g_{k,k,n}=\hat{g}_{k,k,n}+e_{k,k,n}$ and using the fact that MMSE estimate is uncorrelated with the estimation error. Equality (b) is because $\mathbb{E}(\|\hat{\mathbf{h}}_k\|^2)=\delta_k$ and the magnitude $|\hat{g}_{k,k,n}|$ is rice distributed as $\mathrm{Rice}(|\overline{g}_{k,k,n}|,\sqrt{\frac{\upsilon_{k,k,n}}{2}})$, whose first moment is given by $\mathbb{E}(|\hat{g}_{k,k,n}|)=\sqrt{\frac{\pi}{2}}\sqrt{\upsilon_{k,k,n}/2}L_{\frac{1}{2}}(-|\overline{g}_{k,k,n}|^2/\upsilon_{k,k,n})$, where $L_{\frac{1}{2}}(\cdot)$ denotes the Laguerre polynomial function [11, 13.6.9]. Equality (c) is obtained by substituting the expression of $\tilde{\mu}_k$ as in (25). We now consider the term $\overline{I}_{k,n}^{(0)}$ and simplify it as

$$\overline{I}_{k,n}^{(0)}\overset{(a)}{=}\mu_k^2p_{k,n}\left\{\mathbb{E}\left[\left|f_{k,n}g_{k,k,n}\right|^2\right]\mathbb{E}\left[\left|\mathbf{h}_k^T\mathbf{w}_k\right|^2\right]-A_{k,n}\right\}$$
$$\overset{(b)}{=}\mu_k^2p_{k,n}\underbrace{\left\{\left(\left|\overline{g}_{k,k,n}\right|^2+\gamma_{g_{k,k,n}}\right)(\rho_{k,k}+\xi_{k,k})-A_{k,n}\right\}}_{C_{k,n}^{(0)}}$$
$$\overset{(c)}{=}C_{k,n}^{(0)}p_{k,n}\tilde{\mu}_k^2. \quad (26)$$

Equality (a) is due to the statistical independence between $\mathbf{h}_k$ and $g_{k,k,n}$. Equality (b) is because $\mathbb{E}[\mathbf{h}_k^T\mathbf{w}_k]=\sqrt{\delta_k}$, $\mathbb{E}(|\mathbf{h}_k^T\mathbf{w}_k|^2)=(\rho_{kk}+\xi_{kk})$, $\mathbb{E}(f_{k,k,n}g_{k,k,n})=\frac{\sqrt{\pi}}{2}\upsilon_{k,k,n}L_{\frac{1}{2}}\left(\frac{-|\overline{g}_{k,k,n}|^2}{\upsilon_{k,k,n}}\right)$ and $\mathbb{E}(|f_{k,n}g_{k,k,n}|^2)=\mathbb{E}(\frac{|\hat{g}_{k,k,n}|^2|g_{k,k,n}|^2}{|\hat{g}_{k,k,n}|^2})=\mathbb{E}(|g_{k,k,n}|^2)=|\overline{g}_{k,k,n}|^2+\gamma_{g_{k,k,n}}$. We can similarly simplify the interference terms $\overline{I}_{k,n}^1,\cdots,\overline{I}_{k,n}^5$ to obtain the simplified expression in Theorem 1. The expressions of $C_{k,n}^{(1)}$, $C_{k,n}^{(2)}$, $C_{k',k,n}^{(3)}$ and $C_{\substack{k',k'',n'\\k,n}}^{(4)}$ are given as $C_{k,n}^{(1)}=\left(\left|\overline{g}_{k,k,n}\right|^2+\gamma_{g_{k,k,n}}\right)(\rho_{kk}+\xi_{kk})$, $C_{k,n}^{(2)}=\left(\left|\overline{g}_{k,k,n}\right|^2+\gamma_{g_{k,k,n}}\right)(\rho_{k,k}+\xi_{k,k})-\delta_k\left(\left|\overline{g}_{k,k,n}\right|^2+\upsilon_{k,k,n}\right)$, $C_{k',k,n}^{(3)}=\left(|\overline{g}_{k',k,n}|^2+\gamma_{g_{k',k,n}}\right)(\rho_{k',k'}+\xi_{k',k'})$ and $C_{\substack{k',k'',n'\\k,n}}^{(4)}=\left(\left|\overline{g}_{k',k,n}\right|^2+\gamma_{g_{k',k,n}}\right)\rho_{k',k''}$.

REFERENCES

[1] A. S. de Sena, F. R. M. Lima, D. B. da Costa, Z. Ding, P. H. J. Nardelli, U. S. Dias, and C. B. Papadias, "Massive MIMO-NOMA networks with imperfect SIC: design and fairness enhancement," *IEEE Trans. Wireless Commun.*, vol. 19, no. 9, pp. 6100–6115, 2020.

[2] D. Kudathanthirige and G. A. A. Baduge, "NOMA-aided multicell downlink massive MIMO," *IEEE J. Sel. Topics Signal Process.*, vol. 13, no. 3, pp. 612–627, 2019.

[3] L. Sanguinetti, E. Björnson, and J. Hoydis, "Toward massive MIMO 2.0: Understanding spatial correlation, interference suppression, and pilot contamination," *IEEE Trans. Commun.*, vol. 68, no. 1, pp. 232–257, Jan. 2020.

[4] Ö. Özdogan, E. Björnson, and E. G. Larsson, "Massive MIMO with spatially correlated Rician fading channels," *IEEE Trans. Commun.*, vol. 67, no. 5, pp. 3234–3250, 2019.

[5] X. Chen, R. Jia, and D. W. K. Ng, "The application of relay to massive non-orthogonal multiple access," *IEEE Trans. Commun.*, vol. 66, no. 11, pp. 5168–5180, 2018.

[6] V. Mandawaria, E. Sharma, and R. Budhiraja, "Energy-efficient massive MIMO multi-relay NOMA systems with CSI errors," *IEEE Trans. Commun.*, vol. 68, no. 12, pp. 7410–7428, 2020.

[7] Y. Li and G. A. A. Baduge, "Relay-aided downlink massive MIMO NOMA with estimated CSI," *IEEE Trans. Veh. Technol.*, vol. 70, no. 3, pp. 2258–2271, 2021.

[8] J. Zhang, J. Fan, B. Ai, and D. W. K. Ng, "NOMA-based cell-free massive MIMO over spatially correlated rician fading channels," in *2020 IEEE Int. Conf. on Commun., ICC 2020, Dublin, Ireland, June 7-11, 2020*. IEEE, 2020, pp. 1–6.

[9] S. M. Kay, *Fundamentals of Statistical Signal Processing: Estimation Theory*. Prentice Hall, 1997.

[10] E. Björnson, J. Hoydis, and L. Sanguinetti, "Massive MIMO Networks: Spectral, energy, and hardware efficiency," *Foundations and Trends® in Signal Processing*, vol. 11, no. 3-4, pp. 154–655, 2017.

[11] M. Abramowitz and I. A. Stegun, *Handbook of Mathematical Functions with Formulas, Graphs, and Mathematical Tables*, ninth dover printing ed. New York: Dover, 1964.